

PAPER • OPEN ACCESS

## Propagation of elastic solitons in chains of pre-deformed beams

To cite this article: Bolei Deng *et al* 2019 *New J. Phys.* **21** 073008

View the [article online](#) for updates and enhancements.



**IOP** | ebooks™

Bringing you innovative digital publishing with leading voices to create your essential collection of books in STEM research.

Start exploring the collection - download the first chapter of every title for free.



## PAPER

**Propagation of elastic solitons in chains of pre-deformed beams**

## OPEN ACCESS

RECEIVED  
8 March 2019REVISED  
8 May 2019ACCEPTED FOR PUBLICATION  
10 June 2019PUBLISHED  
1 July 2019

Original content from this work may be used under the terms of the [Creative Commons Attribution 3.0 licence](#).

Any further distribution of this work must maintain attribution to the author(s) and the title of the work, journal citation and DOI.

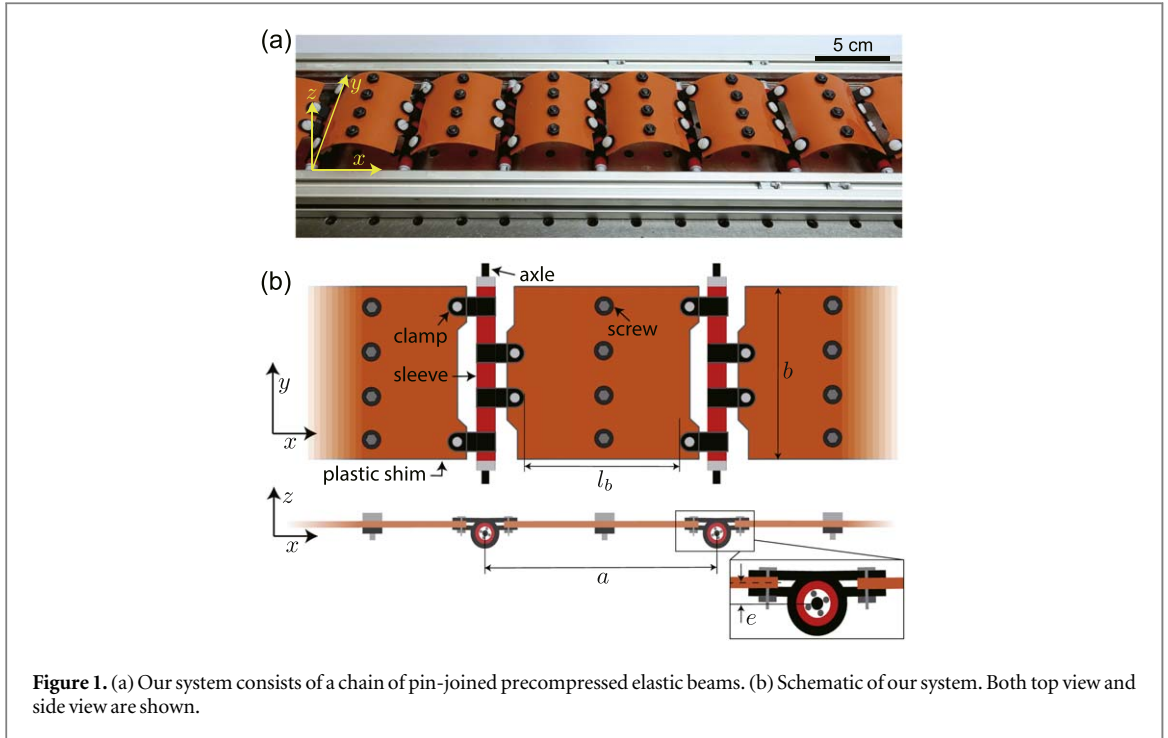
Bolei Deng<sup>1</sup> , Yuning Zhang<sup>2</sup>, Qi He<sup>3</sup>, Vincent Tournat<sup>1,4</sup>, Pai Wang<sup>1</sup> and Katia Bertoldi<sup>1,5</sup><sup>1</sup> Harvard John A. Paulson School of Engineering and Applied Science, Harvard University, Cambridge, MA 02138, United States of America<sup>2</sup> College of Engineering, Peking University, Beijing 100871, People's Republic of China<sup>3</sup> School of Aerospace Engineering, Tsinghua University, Beijing 100084, People's Republic of China<sup>4</sup> LAUM UMR 6613 CNRS, Le Mans University, 72085 Le Mans, France<sup>5</sup> Kavli Institute, Harvard University, Cambridge, Massachusetts 02138, United States of AmericaE-mail: [bertoldi@seas.harvard.edu](mailto:bertoldi@seas.harvard.edu)**Keywords:** solitary waves, elastic beam, nonlinear wavesSupplementary material for this article is available [online](#)**Abstract**

We use a combination of experiments, numerical analysis and theory to investigate the nonlinear dynamic response of a chain of precompressed elastic beams. Our results show that this simple system offers a rich platform to study the propagation of large amplitude waves. Compression waves are strongly dispersive, whereas rarefaction pulses propagate in the form of solitons. Further, we find that the model describing our structure closely resembles those introduced to characterize the dynamics of several molecular chains and macromolecular crystals, suggesting that our macroscopic system can provide insights into the effect of nonlinear vibrations on molecular mechanisms.

**1. Introduction**

Following the seminal numerical experiment of Fermi–Pasta–Ulam–Tsingou [1], which was related by Zabusky and Kruskal to the propagation of solitons [2], a variety of model equations, solution methods and experimental platforms have been developed to investigate the dynamics of discrete and nonlinear one-dimensional mechanical systems across many scales [3–8]. At the macroscopic scale, propagation of solitary waves has been observed in a variety of nonlinear mechanical systems, including chains of elastic beads [9–14], tensegrity structures [15], origami chains [16], wrinkled and creased helicoids [17] and flexible architected solids [18–21]. Moreover, it has been found that even at the molecular scale solitons affect the properties of a variety of one-dimensional structures, including macromolecular crystals [22], polymer chains [23–26], DNA and protein molecules [27–30]. Since detailed experimental investigation of the dynamic behavior of these microscopic systems is limited by their scale, the identification of macroscale structures capable of describing their response is of particular interest as those offer opportunities to visualize the underlying molecular mechanisms.

In this work, we focus on a chain of pin-joined elastic beams subjected to homogeneous static precompression and use a combination of experiments, numerical simulations and theoretical analyses to investigate the propagation of nonlinear pulses. We find that, while large amplitude rarefaction waves propagate in the chain with constant velocity while conserving their spatial shape, the excited compression waves are strongly dispersive. Further theoretical analysis via a continuum model reveals that the system supports solitary solution only for rarefaction pulses—a behavior that roots from the softening behavior of the beams upon compression. Remarkably, we also find that the model describing our system closely resembles those introduced to characterize the dynamics of several molecular chains and macromolecular crystals [22, 24–26]. As such, since the propagation of pulses in our system can be easily visualized, we envision our model to provide opportunities to elucidate how nonlinear vibrations and pre-deformation affect the macroscopic properties of polymers and other macro-molecular chains.



## 2. Experiments

Our sample consists of a long chain of  $N = 40$  elastic beams free to rotate at their ends, but constrained to move only in longitudinal direction (see figure 1(a)). All beams are made of polyester plastic sheets (Artus Corporation, NJ) and have thickness  $t = 0.75$  mm, length  $l_b = 50$  mm, width  $b = 60$  mm and Young's modulus  $E = 4.3$  GPa. Four pairs of screws and nuts are added along their middle line to increase their mass, therefore reducing the speed of the propagating pulses and facilitating their tracking (see figures 1(a), (b)). Moreover, both ends of the beams are connected via plastic clamps (McMaster-Carr part number 8876T11) to LEGO axles (LEGO part number 3708) covered by sleeves (LEGO part number 62462 and 6590) that serve as hinges. The resulting unit cell has length  $a = 75$  mm and the beam offset by a distance  $e = 5.2$  mm from the the line of action of the applied axial load (see figure 1(b)). Finally, to constrain the chain to move only in longitudinal direction, all LEGO hinges are confined to slide in a metallic rail, lubricated to minimize friction.

All our experiments consist of two steps and are conducted on the chain with the left-end connected to a heavy and rigid body and the right-one fixed (see figure 2(c)). First, we compress the structure by slowly moving the heavy rigid body at the left end towards the right by a distance  $\Delta x$ . Such applied displacement induces a longitudinal pre-strain

$$\varepsilon_{st} = -\frac{\Delta x}{N a}, \quad (1)$$

in all beams (with only small variations of  $\sim 5\%$  between the units along the chain) and bends them (see figure 2(a)). In figure 2(b) we show the experimentally measured force required to apply a pre-strain  $\varepsilon_{st}$  to our beams. We find that the response of the beams is continuous (buckling snap-through is absent due to the eccentricity  $e$ ) and that their stiffness monotonically decreases as the precompression increases. As such, our pre-deformed elastic units exhibit a strain-softening behavior if further compressed and a strain-hardening response under stretching.

Second, we initiate an elastic pulse at the left end of the precompressed chain. We strike the heavy rigid body with a hammer toward the right to excite compression pulses, whereas we simply release the rigid body to generate rarefaction pulses (see figure 2(c)). We then record the elastic wave propagation through the first 30 units of the chain with a digital camera (SONY RX100) at 480 fps (see movie S1 is available online at [stacks.iop.org/NJP/21/073008/mmedia](http://stacks.iop.org/NJP/21/073008/mmedia)) and use digital image correlation [31, 32] to monitor the displacement  $q_i$  (see figure 2(c)) of the  $i$ th hinge induced by the pulse. Finally, we calculate the longitudinal strain induced by the propagating pulse in the  $i$ th beam as

$$\varepsilon_i = \frac{q_{i+1} - q_i}{a_{st}}, \quad (2)$$

where  $a_{st} = (1 + \varepsilon_{st})a$  is the unit cell length after precompression.

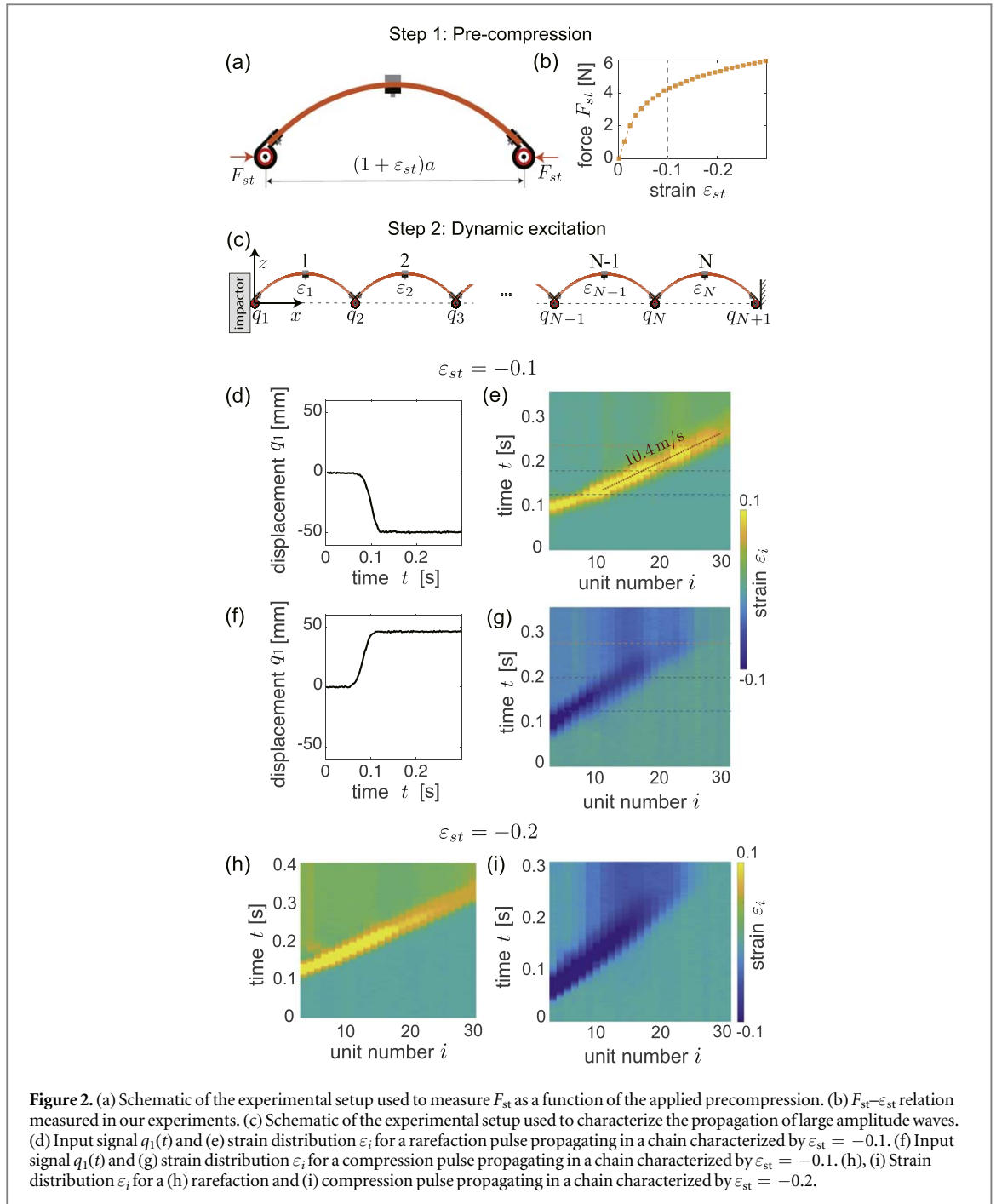
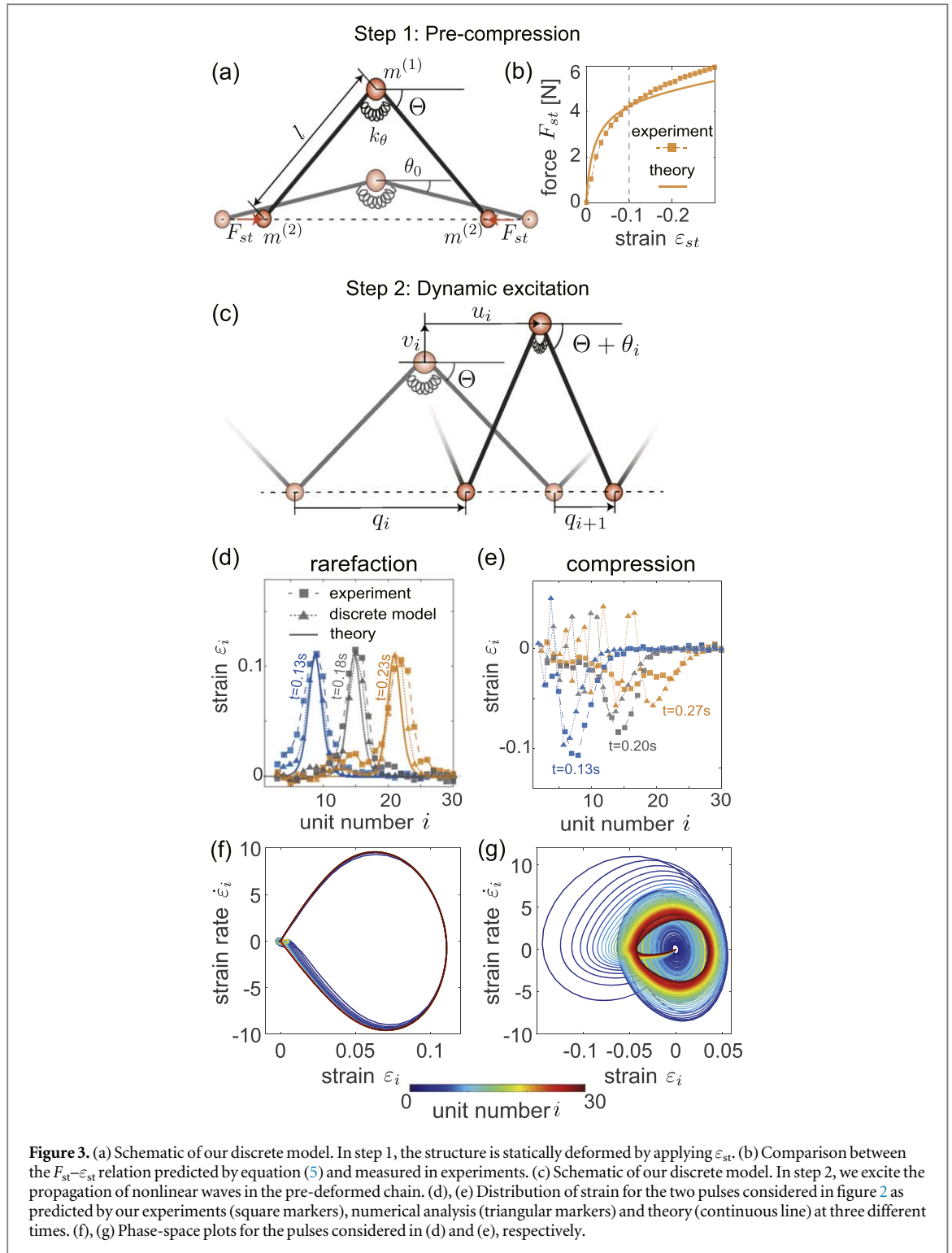


**Figure 2.** (a) Schematic of the experimental setup used to measure  $F_{st}$  as a function of the applied precompression. (b)  $F_{st}$ – $\varepsilon_{st}$  relation measured in our experiments. (c) Schematic of the experimental setup used to characterize the propagation of large amplitude waves. (d) Input signal  $q_1(t)$  and (e) strain distribution  $\varepsilon_i$  for a rarefaction pulse propagating in a chain characterized by  $\varepsilon_{st} = -0.1$ . (f) Input signal  $q_1(t)$  and (g) strain distribution  $\varepsilon_i$  for a compression pulse propagating in a chain characterized by  $\varepsilon_{st} = -0.1$ . (h), (i) Strain distribution  $\varepsilon_i$  for a (h) rarefaction and (i) compression pulse propagating in a chain characterized by  $\varepsilon_{st} = -0.2$ .

In figures 2(d)–(g) we focus on two different experiments conducted on a chain pre-compressed by applying  $\varepsilon_{st} = -0.1$  and report both the displacement signal prescribed by the impactor to the first joint,  $q_1(t)$ , and the spatio-temporal evolution of the strain  $\varepsilon_i$ . We find that, when we initiate a rarefaction pulse (see figure 2(d)), the wave propagates in a solitary fashion, maintaining both its shape (with an amplitude  $\max(\varepsilon_i) \sim 0.11$ ) and velocity ( $\sim 10.4 \text{ m s}^{-1}$ —see figure 2(e)). By contrast, when the impact moves the first beam rightwards (see figure 2(f)), the excited compression pulse disperses as it travels through the structure (see figure 2(g)). As such, in full agreement with previous studies on mechanical chains exhibiting strain-softening [16, 33], our experimental results suggest that large amplitude rarefaction waves are stable, whereas compression pulses disperse. Finally, we want to point out that, while the experimental results reported in figures 2(d)–(g) are for a chain with a pre-strain  $\varepsilon_{st} = -0.1$ , qualitatively similar behaviors are observed in our tests for  $\varepsilon_{st} = -0.2$  (see figures 2(h), (i)). However, using our setup we could not test propagation of pulses in chains subjected to larger compressive pre-strains, as these result in failure of the beams.



### 3. Discrete model

To test the validity of our experimental observations, we establish a discrete model in which each elastic beam is modeled as two rigid rods with length  $l = \sqrt{e^2 + a^2/4} = 38$  mm initially rotated by a small angle  $\theta_0 = \arctan(2e/a) = 0.14$  to account for the eccentricity  $e$  (see figure 3(a)). Each pair of rods is connected at the center by a rotational spring with stiffness  $k_\theta = EI/l_b = 0.22$  Nm ( $I = bt^3/12$  being the area moment of inertia of the beams) that captures the bending stiffness of the elastic beams, while their other two ends are free to slide and rotate (see figure 3(a)). Moreover, we assume that the mass  $m$  of the beams is concentrated at the ends of the rigid rods. Specifically, we place a mass  $m^{(1)} = \alpha m$  at the ends connected by the torsional spring (with  $\alpha \in [0, 1]$ ) and two masses  $m^{(2)} = (1 - \alpha)m/2$  at the other ends (see figure 3(a)). Since in our structure the mass of the beams, hinges and screws/nuts is 3 g, 7 g and 8 g, we find that for the considered system  $m = 18$  g and  $\alpha = 0.56$ . It

should also be noted that our discrete model is similar to the one proposed to describe solitons propagation in polyethylene macromolecules [24–26], providing an interesting analogy between mechanical beams and molecular units.

Identically to our experiments, all our simulations consists of two steps. In the first step we statically compress the structure by reducing the unit cell length to  $a(1 + \varepsilon_{st})$  (see figure 3(a)). Such reduction in unit cell length increases the angle between all rods and the horizontal line from  $\theta_0$  to

$$\Theta = \theta_0 + \theta_{st}, \quad (3)$$

where  $\theta_{st}$  is the rotation induced by the precompression, which can be expressed as a function of  $\varepsilon_{st}$  using

$$\cos \Theta = \frac{a}{2l}(1 + \varepsilon_{st}). \quad (4)$$

Note that the precompression of the beams requires application of a force  $F_{st}$  that satisfies

$$F_{st} l \sin \Theta - k_{\theta} \theta_{st} = 0. \quad (5)$$

In figure 3(b) we compare the  $F_{st}$ – $\varepsilon_{st}$  relation predicted by equations (3)–(5) with experimental measurements and find that the static response of the beams is well captured by the discrete model.

In the second step, we then simulate the propagation of nonlinear waves in the pre-deformed chain (see figure 3(c)). To this end, we define the Lagrangian of the system

$$L = \sum_{i=1}^N \frac{1}{2} m^{(1)} (u_i^2 + v_i^2) + \frac{1}{2} m^{(2)} \dot{q}_i^2 - \frac{1}{2} k_{\theta} (2\theta_{st} + 2\theta_i)^2, \quad (6)$$

where  $u_i$  and  $v_i$  are the longitudinal and transverse displacements of the  $i$ th mass  $m^{(1)}$  excited by the pulse and  $\theta_i$  denotes the wave-induced rotation of the  $i$ th pair of rods (see figure 3(c)). Since in our discrete model each unit has only one degree of freedom,  $u_i$ ,  $v_i$  and  $\theta_i$  can be expressed as a function of the longitudinal displacement of the hinges,  $q_i$ , as

$$u_i = \frac{1}{2}(q_{i+1} + q_i), \quad (7a)$$

$$v_i = \sqrt{l^2 - \left( \frac{q_{i+1} - q_i + 2l \cos \Theta}{2} \right)^2} - l \sin \Theta, \quad (7b)$$

$$\theta_i = \arccos \left( \frac{q_{i+1} - q_i}{2l} + \cos \Theta \right) - \Theta. \quad (7c)$$

By using equations (7), (6) can be written only in terms of  $q_i$  and  $\dot{q}_i$ , and the discrete motion equations of the system can then be obtained via the Euler–Lagrange equations as

$$\frac{d}{dt} \left[ \frac{\partial L(q_i, \dot{q}_i)}{\partial \dot{q}_i} \right] - \frac{\partial L(q_i, \dot{q}_i)}{\partial q_i} = 0, \quad i = 1, \dots, N. \quad (8)$$

For a chain comprising  $N$  beams, equation (8) result in a system of  $N$  coupled differential equations, which we numerically solve using the 4th order Runge–Kutta method (via the Matlab function `ode45`—see supporting information for the Matlab code). To test the relevance of our discrete model, in figures 3(d) and (e) we focus on the two tests presented in figure 2 and compare the evolution of  $\varepsilon_i$  along the chain as extracted from experiments (square markers) and simulations (triangular markers) at three different times. Moreover, in figures 3(f) and (g) we show the numerically obtained phase-space plots for the two pulses. Note that in our numerical analysis we consider a chain comprising  $N = 40$  units, assign  $\varepsilon_{st} = -0.1$  to all beams (as in our experiments), apply the experimentally extracted displacement signal  $q_1(t)$  (see figures 2(d) and (f)) to the first beam and implement fixed boundary conditions at the right end. Remarkably, the numerical results nicely capture the behavior observed in our experiments. As shown in figure 3(d), the numerical analyses indicate that the excited rarefaction pulse propagates without apparent distortion with a velocity of  $\sim 9.8 \text{ m s}^{-1}$ . This prediction is very close to the experimentally measured value of  $\sim 10.4 \text{ m s}^{-1}$ —with the discrepancy mostly arising because our simple model underestimates the stiffness of the beams upon loading (see figure 3(a)). Moreover, the phase-space plot for rarefaction shows a clear homoclinic orbit (see figure 3(f)), which is consistent with a solitary wave solution. By contrast, the compressive pulse is not stable (see figure 3(e))—a feature that is also captured by the chaotic trajectories emerging in the phase-space plot (see figure 3(g)).

#### 4. Continuum model

Having verified the validity of our discrete model, we then simplify equations (8) to derive an analytical solution. To this end, we first introduce a continuous function  $q$  that interpolates the discrete variables  $q_i$  as

$$q(x = x_i) = q_i, \tag{9}$$

where  $x_i = (i - 1)a_{st}$  denotes the position of the left end of the  $i$ th beam in the chain after static precompression. Then, we assume that: (I)  $\varepsilon_i \ll 1$ , so that equations (7b) and (7c) can be approximated as

$$\begin{aligned} v_i &\approx -\frac{q_{i+1} - q_i}{2 \tan \Theta} - \frac{(q_{i+1} - q_i)^2}{8l \sin^3 \Theta}, \\ \theta_i &\approx -\frac{q_{i+1} - q_i}{2l \sin \Theta} - \frac{\cos \Theta (q_{i+1} - q_i)^2}{8l^2 \sin^3 \Theta}, \end{aligned} \tag{10}$$

and (II) the width of the propagating pulse is much larger than the unit cell length  $a$ , so that the displacement of the  $(i - 1)$ th and  $(i + 1)$ th joints can be expressed using Taylor expansion as

$$\begin{aligned} q_{i+1} &\approx \left( q + a_{st}q_x + \frac{a_{st}^2}{2}q_{xx} + \frac{a_{st}^3}{6}q_{xxx} + \frac{a_{st}^4}{24}q_{xxxx} \right) \Big|_{x=x_i} \\ q_{i-1} &\approx \left( q - a_{st}q_x + \frac{a_{st}^2}{2}q_{xx} - \frac{a_{st}^3}{6}q_{xxx} + \frac{a_{st}^4}{24}q_{xxxx} \right) \Big|_{x=x_i}, \end{aligned} \tag{11}$$

where  $q_x = \partial q / \partial x$ . Substitution of equations (10), (11) into equation (8) yields the continuum governing equation

$$\begin{aligned} q_{tt} &= c_0^2(1 - \theta_{st} \cot \Theta) \left( q_{xx} + \frac{l^2}{12} q_{xxxx} \right) + \alpha l^2(\cot^2 \Theta - 1) q_{ttxx} / 4 \\ &+ c_0^2(3 \cot \Theta - \theta_{st} - 3\theta_{st} \cot^2 \Theta) \cot \Theta q_x q_{xx}, \end{aligned} \tag{12}$$

where  $c_0 = 2a_{st} \cot \Theta \sqrt{k_\theta / m}$  denotes the characteristic velocity of the system. Finally, we take the derivative of equation (12) with respect to  $x$  and then introduce the continuum strain distribution  $\varepsilon = \partial q / \partial x$  to obtain

$$\begin{aligned} \varepsilon_{tt} &= c_0^2(1 - \theta_{st} \cot \Theta) \left( \varepsilon_{xx} + \frac{l^2}{12} \varepsilon_{xxxx} \right) + \alpha l^2(\cot^2 \Theta - 1) \varepsilon_{ttxx} / 4 \\ &+ \frac{c_0^2}{2}(3 \cot \Theta - \theta_{st} - 3\theta_{st} \cot^2 \Theta) \cot \Theta (\varepsilon^2)_{xx}, \end{aligned} \tag{13}$$

which has the form of a double-dispersion Boussinesq equation [34] with the double-dispersion term  $\varepsilon_{ttxx}$  introduced because of the inertia coupling between  $m^{(1)}$  and  $m^{(2)}$  (if  $m^{(1)} = 0$ , then  $\alpha = 0$  and the coefficient in front of  $\varepsilon_{ttxx}$  vanishes). Note that the double-dispersion Boussinesq equation was first derived by Boussinesq in the 19th century to account for both the horizontal and vertical flow velocity in the description of nonlinear water waves [34] and has subsequently been used to describe nonlinear waves in a variety of systems, including microstructured solids [35, 36] and polyethylene [24].

Remarkably, it has been shown that the Boussinesq equation admits the solitary wave solution [37, 38]

$$\varepsilon = A \operatorname{sech}^2 \left( \frac{x - ct}{W} \right), \tag{14}$$

where  $c$  is the velocity of the pulse and  $A$  and  $W$  are its amplitude and characteristic width, which are given by

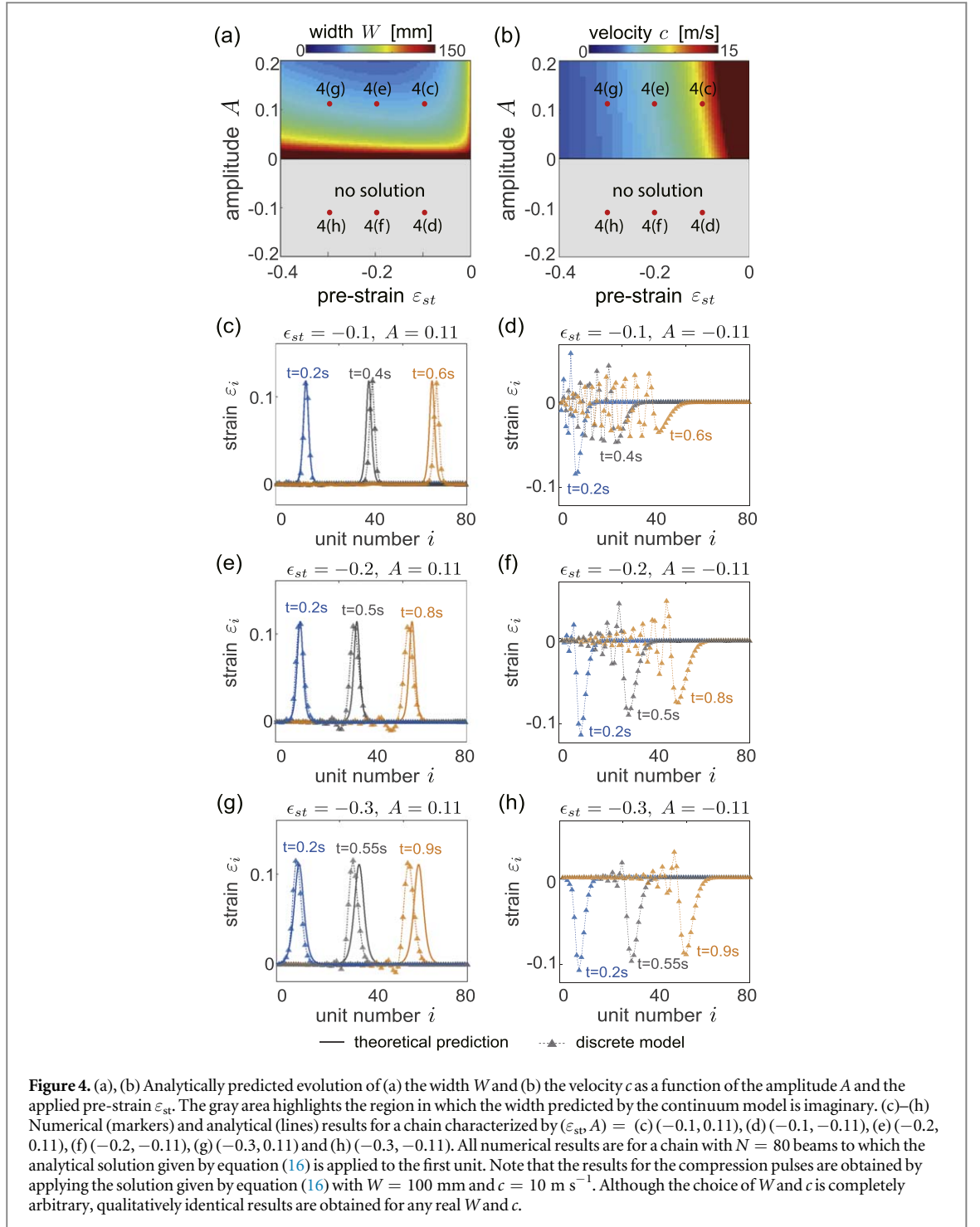
$$\begin{aligned} A &= \frac{3(c^2 - c_0^2 + c_0^2 \theta_{st} \cot \Theta)}{c_0^2(3 \cot \Theta - \theta_{st} - 3\theta_{st} \cot^2 \Theta) \cot \Theta}, \\ W &= l \sqrt{\frac{\frac{c_0^2}{3}(1 - \theta_{st} \cot \Theta) + \alpha(\cot^2 \Theta - 1)c^2}{c^2 - c_0^2 + c_0^2 \theta_{st} \cot \Theta}}. \end{aligned} \tag{15}$$

Finally, the displacement distribution  $q(x)$  can be obtained as

$$q(x) = \int \varepsilon(x) dx = AW \tanh \left( \frac{x - ct}{W} \right) + C \tag{16}$$

where  $C$  is the integration constant that is found as  $C = -AW$  by imposing  $q(x \rightarrow \infty) = 0$ .

Using equation (15), we find that for  $A = 0.11$  (i.e. for a pulse with the same amplitude as the one excited in the experiment of figures 2(d) and (e)), a solitary wave with  $c = 9.31 \text{ m s}^{-1}$  and  $W = 91.6 \text{ mm}$  propagates through the system, in good agreement with both our experimental and numerical observations (see figure 3(d)). By contrast, for a compression pulse with  $A = -0.11$  (i.e. for a pulse with the same amplitude as the one excited in the experiment of figures 2(f) and (g)), equation (15) yields an imaginary  $W$ , confirming that our solitary wave solution is not valid anymore.



Having verified the ability of the analytical solutions to capture our experimental observations, we now use it to investigate how the pre-strain  $\epsilon_{st}$  affects the propagation of the pulses. In figures 4(a) and (b) we report the evolution of  $W$  and  $c$  predicted by equation (15) as a function of  $A$  and  $\epsilon_{st}$ . Remarkably, we find that, irrespective of  $\epsilon_{st}$ , our structure supports solitons only if  $A > 0$ . For  $A < 0$  the width  $W$  predicted by equation (15) is an imaginary number and our solitary solution is not anymore valid. We also find that the width  $W$  of the supported rarefaction solitons is mostly affected by the amplitude  $A$ , whereas the pulse velocity  $c$  monotonically decreases with the increase in precompression ( $-\epsilon_{st}$ )—a dependency that is consistent with the strain-softening behavior of the unit cells under compression. Finally, we note that the predictions of our continuum model are in excellent agreement with those obtained by directly integrating the system of ordinary differential equations given by equation (8). As an example, in figures 4(c)–(h) we compare the results given by our continuum and discrete models for  $A = \pm 0.11$  and three different levels of applied pre-strain (i.e.  $\epsilon_{st} = -0.1, -0.2$  and  $-0.3$ ).

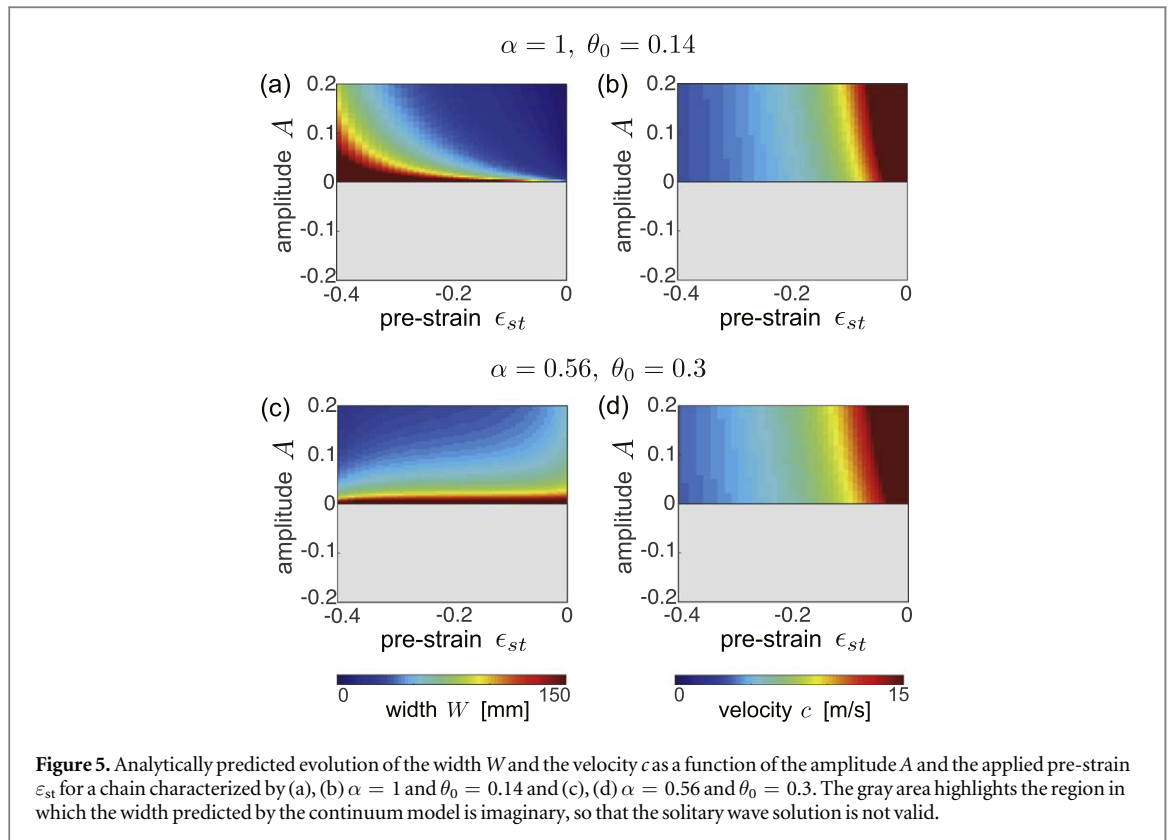


**Figure 5.** Analytically predicted evolution of the width  $W$  and the velocity  $c$  as a function of the amplitude  $A$  and the applied pre-strain  $\epsilon_{st}$  for a chain characterized by (a), (b)  $\alpha = 1$  and  $\theta_0 = 0.14$  and (c), (d)  $\alpha = 0.56$  and  $\theta_0 = 0.3$ . The gray area highlights the region in which the width predicted by the continuum model is imaginary, so that the solitary wave solution is not valid.

The numerical results confirm that only for  $A > 0$  the pulses are stable (and characterized by width and speed very close to those predicted by equation (15)), whereas for  $A < 0$  they are strongly dispersive.

Lastly, we use our analytical solution to investigate the influence of the structural parameters ( $\alpha$ ,  $m$ ,  $k_\theta$  and  $\theta_0$ ) on the characteristics of the supported nonlinear waves. We find that, while  $m$  and  $k_\theta$  (which can be altered by changing the dimensions and material properties of the beams) only affect the characteristic velocity of the system  $c_0 = 2a_{st} \cot \Theta \sqrt{k_\theta/m}$ ,  $\alpha$  (which can be altered by adding or removing screws and nuts along the center line of the beams) and  $\theta_0$  (which can be tuned by changing the offset distance  $e$ ) alter both  $c$  and  $W$  (see figure 5). Furthermore, an exhaustive search in all combinations of structural parameters predicts that nonlinear pulses are stable if and only if  $A > 0$  (see figure 5)—indicating that this system can support rarefaction solitons but not compression ones.

## 5. Conclusions

To summarize, we use a combination of experiments, numerical analyses and theory to investigate the propagation of solitary waves in a 1D chain of precompressed elastic beams. First, we have conducted experiments on a centimeter-scale system to characterize the propagation of large amplitude compression and rarefaction pulses and found that, while the compression pulses disperse, the rarefaction ones retain their shape and propagate with constant velocity. Second, we have derived a continuum model that captures the experimental observations and confirms that the system supports rarefaction solitons only. It is important to emphasize that such behavior is consistent with the static behavior of the precompressed beams (see figure 3(b)), since it has been shown that a chain of units exhibiting softening behavior only supports the propagation of rarefaction solitary waves [33].

This study represents the first step towards the investigation of large amplitude waves in beam lattices in 2D and 3D. While periodic lattices have recently attracted considerable interest because of their ability to tailor the propagation of linear elastic waves through directional transmissions and band gaps (frequency ranges of strong wave attenuation) [39–43], comparatively little is known about their nonlinear behaviors under high-amplitude impacts [20]. The results presented in this paper provide useful guidelines for future explorations of the propagation of nonlinear waves in lattice materials. Finally, since the derived model shares strong similarities with those established to describe the dynamics of polymer and macromolecular crystals [22–27], we believe that our experimental platform (which gives direct access to all parameters and variables of the system) could provide insights into a range of nonlinear wave effects relevant at the molecular scale. In particular, the extension of the

present system to a bistable one in which the beams could bend up and down (in our current setup the bending direction is limited by the surface on which the system is placed) could elucidate the dynamics of topological solitons in polyacetylene [23].

## Acknowledgments

KB acknowledges support from the National Science Foundation under Grant No. DMR-1420570 and EFMA-1741685 and from the Army Research Office under Grant No. W911NF-17-1-0147.

## ORCID iDs

Bolei Deng  <https://orcid.org/0000-0003-2589-2837>

## References

- [1] Fermi E, Pasta P, Ulam S and Tsingou M 1955 Studies of the nonlinear problems *Technical Report* Los Alamos Scientific Lab, New Mexico
- [2] Zabusky N J and Kruskal M D 1965 Interaction of ‘solitons’ in a collisionless plasma and the recurrence of initial states *Phys. Rev. Lett.* **15** 240–3
- [3] Dauxois T and Peyrard M 2006 *Physics of Solitons* (Cambridge: Cambridge University Press)
- [4] Aubry S 1975 A unified approach to the interpretation of displacive and order-disorder systems: I. Thermodynamical aspect *J. Chem. Phys.* **62** 3217–29
- [5] Aubry S 1976 A unified approach to the interpretation of displacive and order-disorder systems: II. Displacive systems *J. Chem. Phys.* **64** 3392–402
- [6] Krumhansl J and Schrieffer J 1975 Dynamics and statistical mechanics of a one-dimensional model hamiltonian for structural phase transitions *Phys. Rev. B* **11** 3535
- [7] Mikeska H 1980 Nonlinear dynamics of classical one-dimensional antiferromagnets *J. Phys. C: Solid State Phys.* **13** 2913
- [8] Mikeska H-J and Steiner M 1991 Solitary excitations in one-dimensional magnets *Adv. Phys.* **40** 191–356
- [9] Nesterenko V 2013 *Dynamics of Heterogeneous Materials* (Berlin: Springer)
- [10] Sen S, Hong J, Bang J, Avalos E and Doney R 2008 Solitary waves in the granular chain *Phys. Rep.* **462** 21–66
- [11] Theocharis G, Boechler N and Daraio C 2013 *Nonlinear Periodic Phononic Structures and Granular Crystals* (Berlin: Springer) pp 217–51
- [12] Porter M A, Kevrekidis P G and Daraio C 2015 Granular crystals: nonlinear dynamics meets materials engineering *Phys. Today* **68** 44–50
- [13] Kim E, Li F, Chong C, Theocharis G, Yang J and Kevrekidis P G 2015 Highly nonlinear wave propagation in elastic woodpile periodic structures *Phys. Rev. Lett.* **114** 118002
- [14] Chong C, Porter M A, Kevrekidis P and Daraio C 2017 Nonlinear coherent structures in granular crystals *J. Phys.: Condens. Matter* **29** 413003
- [15] Fraternali F, Carpentieri G, Amendola A, Skelton R E and Nesterenko V F 2014 Multiscale tunability of solitary wave dynamics in tensegrity metamaterials *Appl. Phys. Lett.* **105** 201903
- [16] Yasuda H, Miyazawa Y, Charalampidis E G, Chong C, Kevrekidis P G and Yang J 2019 Origami-based impact mitigation via rarefaction solitary wave creation *Sci. Adv.* **5** eaau2835
- [17] Maurin F 2017 Solitary waves in longitudinally wrinkled and creased helicoids *Int. J. Non-Linear Mech.* **89** 13341
- [18] Deng B, Raney J, Tournat V and Bertoldi K 2017 Elastic vector solitons in soft architected materials *Phys. Rev. Lett.* **118** 204102
- [19] Deng B, Wang P, He Q, Tournat V and Bertoldi K 2018 Metamaterials with amplitude gaps for elastic solitons *Nat. Commun.* **9** 3410
- [20] Kim H, Kim E, Chong C, Kevrekidis P and Yang J 2018 Demonstration of dispersive rarefaction shocks in hollow elliptical cylinder chains *Phys. Rev. Lett.* **120** 194101
- [21] Deng B, Tournat V, Wang P and Bertoldi K 2019 Anomalous collisions of elastic vector solitons in mechanical metamaterials *Phys. Rev. Lett.* **122** 044101
- [22] Sumpter B, Noid D, Liang G and Wunderlich B 1994 Atomistic dynamics of macromolecular crystals *Adv. Polym. Sci.* **116** 27–72
- [23] Su W, Schieffer J and Heeger A 1980 Soliton excitations in polyacetylene *Phys. Rev. B* **22** 2099–111
- [24] Manevitch L I and Savin A V 1997 Solitons in crystalline polyethylene: isolated chains in the transconformation *Phys. Rev. E* **55** 4713–9
- [25] Savin A V and Manevitch L I 1998 Solitons in crystalline polyethylene: a chain surrounded by immovable neighbors *Phys. Rev. B* **58** 386–400
- [26] Savin A V, Manevitch L I, Christiansen P L and Zolotaryuk A 1999 Nonlinear dynamics of zigzag molecular chains *Phys.—Usp.* **42** 245
- [27] Davydov A S 1979 Solitons in molecular systems *Phys. Scr.* **20** 387–94
- [28] Peyrard M and Bishop A R 1989 Statistical mechanics of a nonlinear model for dna denaturation *Phys. Rev. Lett.* **62** 2755
- [29] Peyrard M, Dauxois T, Hoyet H and Willis C 1993 Biomolecular dynamics of dna: statistical mechanics and dynamical models *Physica D* **68** 104–15
- [30] Dauxois T, Peyrard M and Bishop A R 1993 Entropy-driven dna denaturation *Phys. Rev. E* **47** R44
- [31] Senn M 2016 Matlab central file exchange: digital image correlation and tracking <https://mathworks.com/matlabcentral/fileexchange/50994-digital-image-correlation-and-tracking>
- [32] Wadhwa N *et al* 2017 Motion microscopy for visualizing and quantifying small motions *Proc. Natl Acad. Sci.* **114** 11639–44
- [33] Herbold E B and Nesterenko V F 2012 Propagation of rarefaction pulses in particulate materials with strain-softening behavior *AIP Conf. Proc.* **1426** 1447–50
- [34] Boussinesq J 1871 Théorie de l’aintumescence liquide appelée onde solitaire ou de translation se propageant dans un canal rectangulaire *CR Acad. Sci. Paris* **72** 755–9
- [35] Engelbrecht J, Salupere A and Tamm K 2011 Waves in microstructured solids and the boussinesq paradigm *Wave Motion* **48** 717–26

- [36] Berezovski A, Engelbrecht J, Salupere A, Tamm K, Peets T and Berezovski M 2013 Dispersive waves in microstructured solids *Int. J. Solids Struct.* **50** 1981–90
- [37] Christov C I, Maugin G A and Porubov A V 2007 On boussinesq paradigm in nonlinear wave propagation *C. R—Mèc.* **335** 521–35
- [38] Bruzon M 2009 Exact solutions of a generalized boussinesq equation *Theor. Math. Phys.* **160** 894–904
- [39] Phani A S, Woodhouse J and Fleck N 2006 Wave propagation in two-dimensional periodic lattices *J. Acoust. Soc. Am.* **119** 1995–2005
- [40] Wang P, Casadei F, Kang S H and Bertoldi K 2015 Locally resonant band gaps in periodic beam lattices by tuning connectivity *Phys. Rev. B* **91** 020103
- [41] Miniaci M, Krushynska A, Movchan A B, Bosia F and Pugno N M 2016 Spider web-inspired acoustic metamaterials *Appl. Phys. Lett.* **109** 071905
- [42] Bayat A and Gaitanaros S 2018 Wave directionality in three-dimensional periodic lattices *J. Appl. Mech.* **85** 011004
- [43] Wang P, Zheng Y, Fernandes M C, Sun Y, Xu K, Sun S, Kang S H, Tournat V and Bertoldi K 2017 Harnessing geometric frustration to form band gaps in acoustic channel lattices *Phys. Rev. Lett.* **118** 084302